

A processing method for kinematics data of human knee joint obtained by motion-capture measurement

Jian-Ping Wang

Henan Polytechnic University

Shi-hua Wang

Henan Polytechnic University

Xuan Zhao

Henan Polytechnic University

Hai Hu

Shanghai Sixth Peoples Hospital

Yan-qing Wang

Qiqihar Medical University

Jin-lai Liu

The First Affiliated Hospital of Henan Polytechnic University

Xu Chen

The First Affiliated Hospital of Henan Polytechnic University

Yu Li (✉ wjp.sjtu@gmail.com)

Henan polytechnic university

Research

Keywords: Knee joint, Motion capture measurement, MATLAB, Kinematics

Posted Date: June 17th, 2020

DOI: <https://doi.org/10.21203/rs.3.rs-35434/v1>

License:   This work is licensed under a Creative Commons Attribution 4.0 International License.

[Read Full License](#)

A processing method for kinematics data of human knee joint obtained by motion-capture measurement

Jian-Ping Wang¹, Shi-hua Wang¹, Xuan Zhao¹, Hai Hu², Yan-Qing Wang³, Jin-Lai Liu⁴, Xu Chen⁴, Yu Li^{1,*}

*Correspondence: wjp.sjtu@gmail.com

¹ School of Mechanical and Power Engineering, Henan Polytechnic University, Jiaozuo 454000, China

² Shanghai Sixth People's Hospital, Shanghai 200233, China.

³ Medical University, Qiqihar 161006, Heilongjiang Province, China. School of medical technology.

⁴ The First Affiliated Hospital of Henan Polytechnic University, Jiaozuo 454000, Henan Province, China.

Abstract

Background: The data obtained by motion capture method is many and complex, so it is the key to find an efficient method to process the data. Therefore, to develop a processing method for kinematics data of human knee joint by programming on MATLAB software.

Methods: The coordinate data of markers on human lower limb measured by motion capture system were firstly read and repaired through the program. Then the coordinate data of anatomical points in the movement of human lower limb were obtained by program processing. The local coordinate systems of human femur and tibia were established with anatomical points. After that the flexion/extension, abduction/adduction and internal/external rotation of human knee tibiofemoral joint in the movement of lower limb were obtained by coordinate transformation. Lastly, the motion capture and measurement of healthy volunteers were carried out and the MATLAB program was used for data processing.

Results: Using the above methods, motion capture measurements and batch data processing were carried out on squatting and ascending stairs of 29 healthy volunteers to obtain the motion characteristics of the knee joint. As

22 follows, the maximum range of internal and external rotation in squatting is 30.5 degrees, and the maximum range
23 of internal and external rotation in climbing stairs is 16.5 degrees, etc., respectively compared with the results
24 processed by other research methods, it is found that their movement results are basically consistent, thus verifying
25 the reliability of our research method.

26 **Conclusion:** The kinematics data of human knee joint could be processed accurately and effectively with the
27 method by using MATLAB software, and the kinematics characteristics of human knee tibiofemoral joint were
28 obtained. The processing method provides a reference for the designing and optimization of knee prosthesis, and
29 the program can be modified for different purposes. At the same time, it is helpful to study knee joint movement of
30 patients after total knee arthroplasty.

31 **Keywords:** Knee joint, Motion capture measurement, MATLAB, Kinematics

32 **Background**

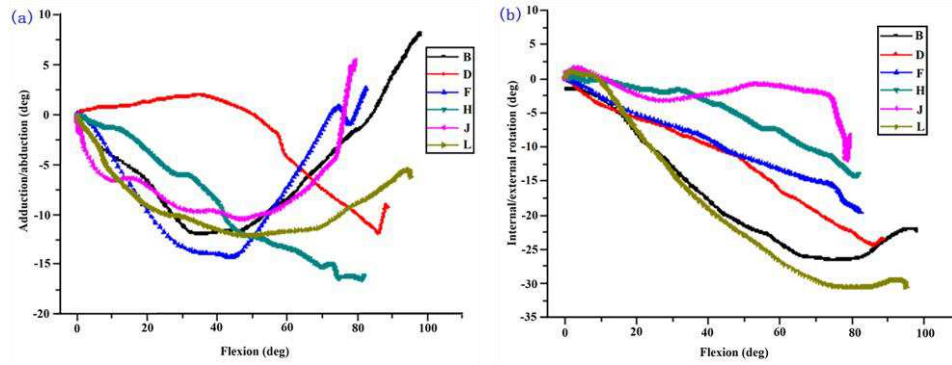
33 Total Knee Arthroplasty (TKA) is a routine procedure used to treat knee-related diseases in
34 humans [1-3]. It replaces the diseased tissue of the knee joint with an artificial joint prosthesis to
35 restore the normal function of the knee joint and improve the quality of life of patients. By
36 measuring the lower limbs of healthy volunteers of a certain species, the anatomical
37 characteristics and movement parameters of the knee were obtained, which can provide reference
38 for the design and optimization of artificial knee prosthesis in line with the characteristics of this
39 species. With the development of motion capture technology [4-6], Some scholars carry out
40 motion capture measurement of human gait [7-9], Some scholars have made motion capture
41 measurement and analysis of human knee joint squatting [10-11], and some scholars use the
42 motion capture system to measure and analyze the motion characteristics of the lower extremity
43 joints during the stair climbing process [12-15], most of them use the commercial motion capture

44 systems such as Visual3D (C-Motion, USA) and Vicon (Oxford Metrics Limited, UK) to calculate
45 and analyze the kinematic parameters of the human knee joint. This method needs to be manually
46 processed one by one, which is time-consuming and labor-intensive [16]. However, through the
47 use of MATLAB (MathWorks, USA), according to the preparation, calibration, and measurement
48 process and characteristics of motion capture measurement, a special program for motion capture
49 measurement can be written, which can batch process motion capture data and customize relevant
50 data tables [17]. In this paper, the motion capture system is used to measure the squat and stair
51 movement of healthy volunteers, and the coordinate data of the body surface markers are
52 obtained; The MATLAB software was then used to design a method for reading and processing
53 the knee joint motion data. The kinematics parameters of the knee femoral tibial joint during the
54 movement of the lower limbs were obtained by data processing.

55 **Result**

56 The method described in this paper was applied to capture and measure the subjects' motion and
57 process the data, so as to obtain the flexion-extension, adduction-abduction, and internal-external
58 rotation data of the knee joint femur relative to the tibia during the movement of the lower limbs.
59 As shown in **Fig. 1** and **Fig. 2**, respectively, the x-coordinate is knee flexion Angle, and the
60 y-coordinate is adduction-abduction and internal-external rotation.

61



62

63 **Fig. 1** (a) The relative rotation motion of femur vs tibia under different flexion during squat (abduction/adduction).

64 (b) The relative rotation motion of femur vs tibia under different flexion during squat (internal/external rotation)

65 **Figure 1** shows the adduction-abduction and internal-external rotation of the human knee joint

66 femur relative to the tibia at different flexion angles during squatting for six healthy subjects. As

67 the knee flexion angle deepens, the femur is abducted and then adducted relative to the tibia, and

68 the femur is always in an external rotation state relative to the tibia. It can be seen from the figure

69 that the maximum flexion angle of the knee joint in the squat is between 79 and 98 degrees, which

70 is smaller than the maximum knee flexion angle of the normal squat motion. The reason is that the

71 experiment and an X-ray stereophotometry experiment (RSA, Roentgen Stereophotogrammetric

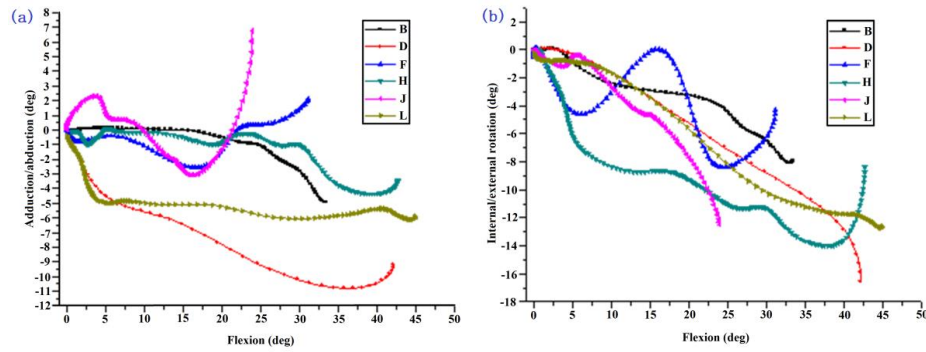
72 Analysis) are synchronized, volunteers' movement space being limited, and the experiment

73 requires volunteers to behave in a specified small action and within 5 seconds shooting times.

74 Accordingly, other knee movement parameters were also relatively small.

75

76



77

78 **Fig.2** (a) The relative rotation motion of femur vs tibia under different flexion during upstairs climbing
 79 (abduction/adduction). (b) The relative rotation motion of femur vs tibia under different flexion during upstairs
 80 climbing (internal/external rotation)

81 **Figure 2** shows the adduction-abduction and internal and external rotation of the femur relative to
 82 the tibia during the ascending step of a healthy subject. Since the experiment was performed in
 83 parallel with the RSA experiment, the volunteers had limited shooting space and a short
 84 measurement time, required to be completed within 5 seconds, and the height of the stairs used for
 85 the measurement was small. Therefore, the maximum flexion angle of the knee joint was smaller
 86 during the stairs climbing. It can be seen from the figure that the maximum flexion angle of the
 87 knee joint of the subject is between 23 and 44 degrees. Due to the higher mobility of the knee joint
 88 on the anterior-posterior axis, as the knee flexion angle increases, the femur with respect to tibia
 89 has a larger difference in adduction and abduction movements; but the femur first abducts and
 90 then adducts overall. At the same time, in the process of going up the stairs, starting from the knee
 91 flexion, the femur continues to be external-rotation with respect to the tibia as a whole. However,
 92 in some subjects, the femur rotates inward at the end of knee flexion.

93 **Discussion**

94 In this paper, the motion capture measurement of the squat and upstairs movements of the subjects
 95 was carried out. The relative movements of the human knee joints in the lower limbs movements

96 were analyzed. For the squatting movement, in the study of Schmitz[10], the squat of 15 healthy
97 people was measured by the motion capture system. The experimental conditions were used to
98 control the flexion angle of the knee joint to 60 degrees, and the data was processed by Visual 3D
99 software. The results showed that in a squat cycle, from the beginning to the flexion angle of the
100 knee joint reaching the maximum, the knee joint was always in external-rotation. This is
101 consistent with the trend of movement in this squat measurement. In the study of Clement[11], 5
102 healthy people and 5 patients with osteoarthritis were compared and analyzed in the quasi-static
103 and dynamic lower knee joint movement. Five flexion positions were selected in the experiment,
104 and the maximum flexion angle was at 72 degrees, the results showed that as the knee flexed, the
105 external-rotation and posterior-translation of the knee increased. This is also consistent with the
106 changes of the knee joint movement in this paper. In the work of many other scholars, the
107 maximum flexion angle of the knee joint in the squatting process exceeded 130 degrees [18-19].
108 The maximum flexion angle of the knee joint in this experimental was smaller, between 79 and 98
109 degrees. And this based on these below reason: This experiment is measured synchronously with
110 the RSA experiment. The volunteers did the movement between the two C-arms, so the shooting
111 space is limited, and in order to ensure that the RSA experiment can capture the human knee joint,
112 the volunteers are required to follow the prescribed action (action range is smaller), and the each
113 measurement time should not exceed 5 seconds.

114 As for the action of stairs climbing, Riener [12] measured the upstairs movements of 10 normal
115 people on the steps with different slopes, and analyzed the joint movement of the lower limbs. The
116 results show that the joint angle is significantly related to the step slope, and the larger the step
117 slope is, the greater the maximum flexion angle of the knee joint during movements is. Tang Gang

118 et al [15] used a staircase with 160 mm in height to analyze the changes of the lower limb joint
119 angle of healthy volunteers during the ascending stairs. It was pointed out that the knee flexion
120 angle range was 91.4 degrees, and the adduction-abduction range was 12.1 degrees, and the
121 rotation range is 20.5 degrees. The height of the stair used in this paper is 100mm, and the greatest
122 knee flexion angle during stairs climbing is 44 degrees. At the meantime, the maximal range of the
123 knee joint adduction-abduction is 10.8 degrees, and the maximum range of internal-external
124 rotation is 16.5 degrees, which is in line with the research results in literature [12], but lower than
125 that in literature [15]. It shows that adduction-abduction and internal-external rotation angle are
126 within a reasonable range, and indicates the reliability and rationality of this experimental results.
127 In this experiment, the patients having been operated shortly after TKA was conducted the same
128 measurement considering the difference in knee joint motion function of patients after surgery, the
129 height of stair steps was required to be low. Besides, RSA (Roentgen Stereophotogrammetric
130 Analysis) and high-speed photographic experimental measurements were also carried out in this
131 experiment to facilitate data control analysis. During the experiment, due to the limited shooting
132 space of experimental equipment and the space limitations caused by the simultaneous
133 measurement of multiple systems, the volunteers' motion range was small and the shooting time
134 could not exceed 5 seconds. Based on the above two main reasons, the maximum buckling Angle
135 of knee joint in the stair climbing experiment in this paper is small.

136 This experiment calibrate the anatomical feature points under the guidance of a professional
137 orthopedist. Multiple calibrations are required prior to formal testing to ensure accurate position of
138 the anatomical feature points. Volunteer require training for actions to enable them to perform as
139 specified. In the formal experiment, each action is measured multiple times, and then the normal

140 behavior of the most normal state is selected for analysis. However, the method described in this
141 paper also has some limitations, for example, the motion capture measurement of human lower
142 extremity motion and the calculation of kinematic parameters of the knee joint need to use the
143 seven anatomical feature points to establish the coordinate system of the femur and tibia.
144 Therefore, the determination of the anatomical feature point position has certain influence on the
145 experimental results.

146 At present, there are a variety of methods for the processing of kinematics data measured by
147 motion capture system and special software for data processing, including the de-noise processing
148 of data, the matching of scattered data and the repair of missing points. Wu sheng [20] proposed a
149 data processing algorithm based on the piecewise linear model of modules, which can effectively
150 carry out global hierarchical prediction and tracking of 3d motion data modules, carry out
151 module-based denoising processing of noise data, and put forward piecewise Newton interpolation
152 operation based on missing motion data to make reasonable supplement. In this paper, cubic spline
153 interpolation function is used to repair the interpolation program. The interpolated curve of this
154 method is second-order continuous and differentiable, and the interpolation operation method of
155 piecewise Newton interpolation has high accuracy and smooth curve transition. AlonsoF.J. Et al.
156 [21] proposed to use the inverse dynamics model of human skeleton for motion data processing,
157 where the complement algorithm based on rigid body requires that there should not be too many
158 defects in the rigid body. For example, for the four waist points, matching complement points can
159 be obtained only when one point is missing, which is the same idea as the repair data in this paper.
160 When one of four marker points missed, it can be repaired; when two or more marker points
161 missed, it cannot be repaired, so it needs to be abandoned. Liu [22] et al. used piecewise linear

162 PCA technology to estimate the missing points and introduced statistical theory into motion data
163 processing for statistical analysis. In terms of motion data processing software, as mentioned in
164 literature [10], Visual3D commercial software and Vicon optical infrared motion capture system
165 [23] were used for data processing of the experimental data of lower limb motion measurement by
166 motion capture system. The system cost a lot. These softwares can automatically analyze and
167 report motion capture data. When the data was of the large sample size, and there are some points
168 being not captured or covered during the movement, it can only be supplemented manually and
169 the data need to be processed manually one by one in these softwares. At the same time, in the
170 initial stage of data processing, everyone needs to use BodyBuilder, a systematic biomechanical
171 modeling software, to model the motion model, which need costing much time. In this paper,
172 MATLAB software is used as a tool to program and process human knee motion capture data.
173 MATLAB program written by this paper can read kinematics data in batches and repair data. The
174 local coordinate system of tibial femur can be established by using bone markers in the program.
175 At last, according to the coordinate transformation, the kinematics parameters of knee femur
176 relative to tibia in the movement of human lower limbs are quickly calculated, and the spatial
177 coordinate curve of knee tibial femur in the movement process also can be obtained. Therefore,
178 human motion can be processed quickly by batch processing, and the program can be modified to
179 meet different special requirements of motion function analysis. In the future, more accurate
180 kinesiology data will be obtained by increasing the sample size and continuously improving the
181 program.

182 **Conclusions**

183 A set of methods was designed to process human knee motion data in this paper, and programs

184 was written in MATLAB software. The kinematics parameters of the femoral tibial joint of the
185 knee joint during squatting and stair climbing were obtained. For the squat movement, when the
186 knee joint reaches the maximum flexion (79-98 degrees) from the beginning of flexion to the
187 maximum flexion angle, the knee femoral tibial joint is always in the external-rotation state during
188 the whole process, and the maximum outward rotation is 30.5 degrees. In this paper, the maximum
189 flexion angle of knee joint in the process of stair climbing is 44 degrees, and the knee femoral
190 tibial joint is also in external-rotation all the time with a maximum of 16.5 degrees, and the range
191 of adduction-abduction is 10.8 degrees. The research results of other researchers are consistent
192 with the movement trend of knee squat and stair climbing in this paper, which also verifies the
193 validity and rationality of the data processing method in this paper. It could be fast, convenient
194 and accurate in processing human knee motion data by using the method in this paper; and the
195 program can be modified according to different research purposes. It can provide data support for
196 the design and optimization of artificial knee prosthesis, provide reference and help for the study
197 of knee movement of patients after TKA and provide data processing for kinematics research of
198 human body.

199 **Methods**

200 **Subjects**

201 There were 29 experimental volunteers, including 17 males and 12 females within 150-178cm
202 height (average 165.5cm) and 47-81kg weight (average 63.9kg). The population of Shanghai
203 urban area were selected as volunteers:15 young volunteers aged 22-28 years old and 14
204 middle-aged volunteers aged 41-71 years old.

205 **Instrumentation**

206 The experiment of motion capture measurement was carried out in Shanghai Sixth People's
207 hospital. The experiment used the Optotrak Certus (NDI, Canada) motion capture system with two
208 position sensors, as shown in **Fig. 3**.



209

210

Fig. 3 Position sensors of motion capture system

211 **The experimental process**

212 In this experiment, only the right leg movement of the volunteers was measured. Then the
213 calibration of the motion capture was performed, which includes: initial calibration the
214 determination of the coordinate system, the calibration of the seven bone markers and the ground
215 reference point. The seven bone markers are respectively the femoral trochanter, the femoral
216 condyle and the medial malleolus, the medial and lateral tibial plateau, and the medial and lateral
217 condyles of ankle joints. In this experiment, the detailed processes, from registering volunteer
218 information and calibration to finally saving data, were shown in **Fig. 4** below.

219

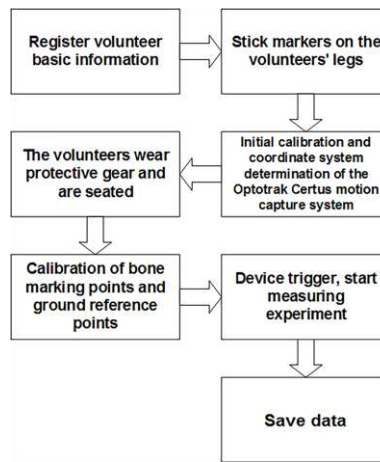


Fig. 4 Motion capture measurement flow chart

As shown in the Fig. 5, there are 4 marks respectively that were placed respectively on the thigh and calf, which were used for motion capturing; and there are 7 anatomical feature points lower limbs and one ground reference points, which were used for calibration to determine the coordinate systems. In order to avoid the measurement error, which caused by skin movement during movements and the bony point being occluded, virtual markers were generally used for calibration measurement [24], these 7 anatomical feature points are just virtual markers for measurement. The coordinates of virtual-Markers in the experiment can be determined by the coordinates of 3 or 4 Marker points photographed on the rigid body. Therefore, the real-time coordinates of anatomical feature points of human lower limbs in the movement can be obtained by measuring the coordinates of markers pasted on volunteers' thighs and calves.

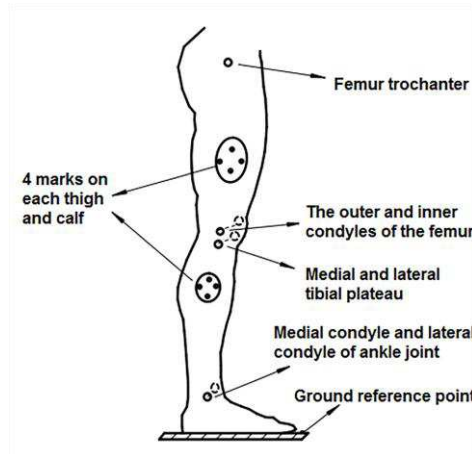


Fig. 5 The position of Markers and anatomic feature points in human lower extremity

Spatial three-dimensional coordinate data of Marker points and bony points were saved by the motion capture system in a file in xls format. Volunteers of the motion capture and measurement of the knee joint squatting and the parts were shown in Fig. 6. Figure 6a shows the initial squat measurement position, when the lower limbs remain upright. Figure 6b is the position with the largest knee flexion angle in the squat. The rest Marker points shown in the figure are coincident markers for other motion measurement, which have no direct relationship with the motion capture measurement in this paper.

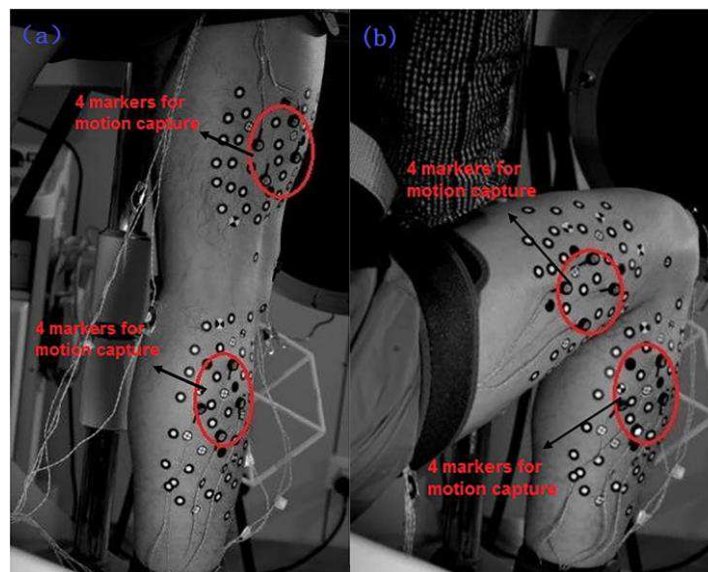
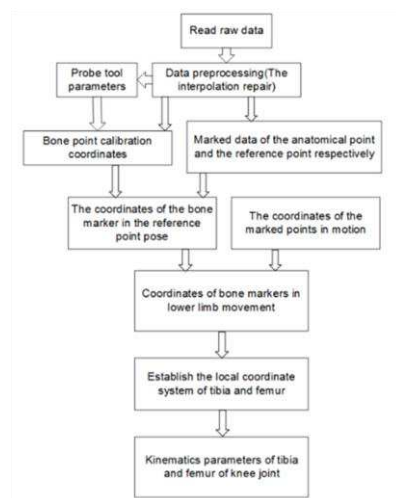


Fig. 6 (a) Site Map of Squatting Motion Measurement (orthostatism). (b) Site Map of Squatting Motion Measurement (maximum of knee joint flexion)

245 **Data processing method**

246 MATLAB software was used to write the program to obtain and analyze the 3D coordinate data of
247 markers. If the collected data were missing, the original data should be first interpolated and
248 repaired reasonably. If the data were intact, it could be read and processed directly. Secondly, the
249 data were processed to obtain the coordinates of 7 anatomical feature points (**Fig. 5**) in the
250 movement of lower limbs, and the local coordinate systems of femur and tibia were established
251 based on these 7 markers. Finally, the kinematics parameters of the knee tibiofemoral joint during
252 the movement of the lower limbs were obtained by using coordinate transformation. The
253 kinematics parameters respectively were below: the flexion and extension of femur relative to
254 tibia, adduction and abduction, and internal and external rotation. The data processing flow chart
255 is shown in **Fig. 7**.



256

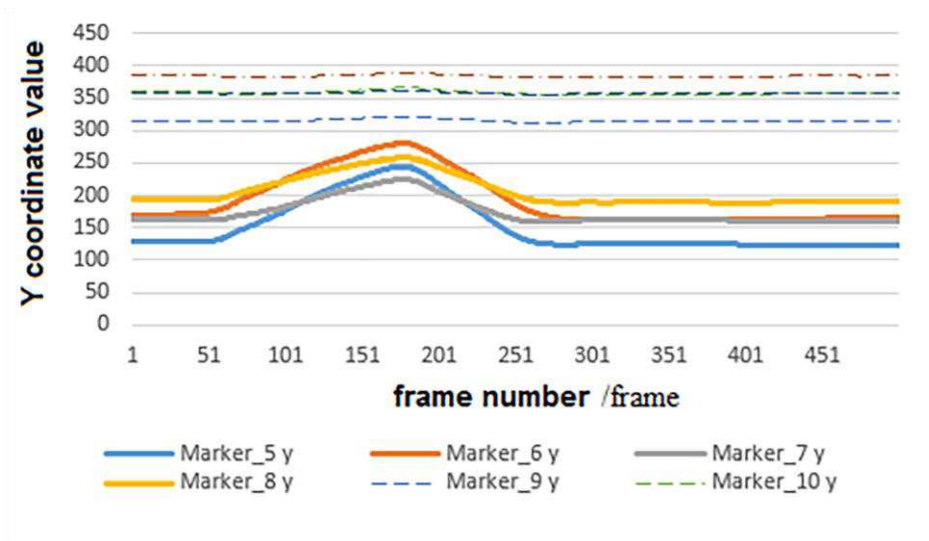
257

Fig. 7 Data processing flow chart

258 **Reading and preprocessing of the original coordinate data of the marker points**

259 The original data measured in the experiment included coordinates during calibration below:
260 markers on the probe tool and markers pasted on the leg for motion capture, and the coordinates of
261 human lower limb movement: the coordinates of marker points on the leg. The data read function

262 'xlsread' was used in the MATLAB software to directly read coordinate data.



263

264

Fig. 8 The coordinate values in Y direction of markers in thigh and shank in a squat

265

Figure 8 shows the change of the coordinate value of the Marker points on the legs in the up

266

and down direction. The horizontal coordinate represents the number of frames. Marker 5-8 is on

267

the thigh, Marker9-12 is on the lower leg, and the data of markers on the lower leg has a small

268

change because of the small amplitude of the calf in the movement. It could be seen that in the

269

first 50 frames, the data remains unchanged. Within these 50 frames, the volunteers do not move,

270

and then the squatting action begins. After reaching the lowest point, the knee began extending

271

and the data appears to be increasing firstly and then decreasing. Finally, the volunteers remained

272

stationary and the data remained unchanged.

273

In the experimental process, some of the coordinate data of markers were missing due to

274

some of them being obscured, and the missing data needs to be repaired. The patch function were

275

programed in Matlab based on the number of missing data and the missing position. As **Fig. 8**

276

shown: within 1-50 frames in the beginning and the last 200 frames, the volunteers were stationary,

277

so the lack of data in these two stages has no effect on the results. It takes 2.5 seconds for 50-300

278

frames to complete the collection from squatting to standing, in which the data-loss will be caused

279 by marker points being obscured or falling during the movement. When one of the 4 markers
280 points (which were on the thigh or calf, as shown in **Fig. 5**) missed, it can be repaired. However, it
281 cannot be repaired and should be discarded when 2 or more markers of the 4 markers missed.

282 The positional correlation among markers during the movement and the overall movement
283 trend are all references for data repair. For example, this relation can be obtained according to the
284 real-time coordinates of the upright position and the maximum flexion position shown in **Fig. 6a**
285 and **Fig. 6b** respectively, and the real-time coordinates of the anatomical feature points of the
286 upright position shown in **Fig. 5**. When the patch program was written, cubic spline interpolation
287 function was used for interpolation repair [25]. The curve after interpolation by this method is
288 second-order continuous and differentiable, with high precision and smooth curve transition. The
289 detailed introduction of cubic spline interpolation function is described in literature [25], and its
290 principle is shown in **Appendix. 1**.

291 The written patch flowchart is shown in **Fig. 9** below. In the experiment, as shown in **Fig. 6**,
292 there are 4 Markers attached to the thighs and calves of the volunteers respectively. If there is one
293 Marker data missing in the nth frame in the motion measurement, then according to the data of 4
294 markers in the previous frame or the nearest frame and the remaining three Marker data of the nth
295 frame, the transformation matrix and a translation matrix between the two sets of coordinates were
296 established, thereby the coordinate data of missing markers in the nth frame were solved.

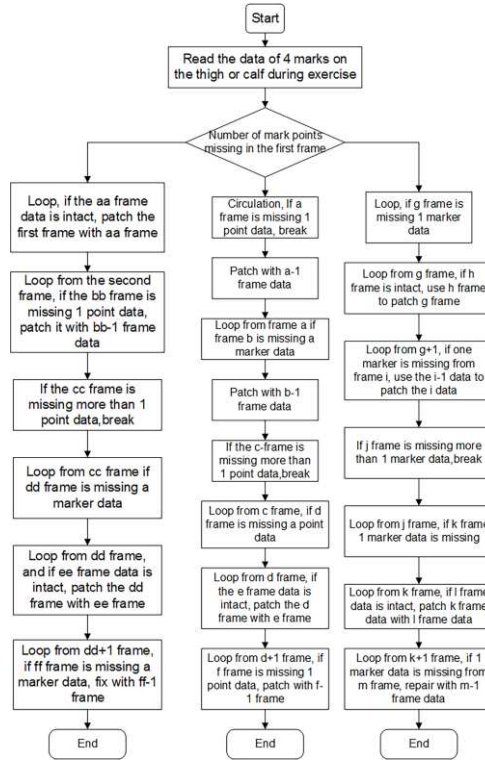


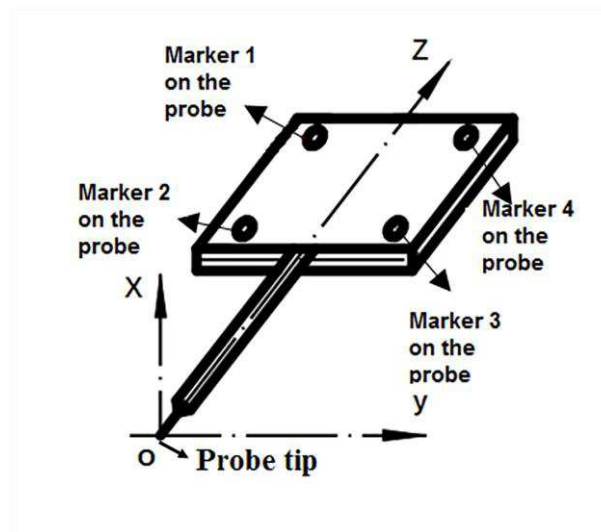
Fig. 9 Patch program flow chart

Solution of Coordinate Data of Bone Markers in Lower Limb Movement

Two sets of three-dimensional point sets $\{p_i\}$ and $\{p_i'\}$ are known, $i=1, 2, \dots, N$, N is the number of markers, $\{p_i\}$ and $\{p_i'\}$ are 3×1 column matrix, then there is $p_i' = Rp_i + T$, where R is the 3×3 rotation matrix, and T is the 3×1 translation vector of the column matrix, The transformation matrix R and the translation matrix T can be solved based on the known two sets of points based on the singular value decomposition method.

Figure 10 shows the probe and probe local coordinate system, the tip of the probe was defined as the local coordinate system origin. According to the coordinate data of 4 marker points on the probe obtained by measurement and the parameters of the probe itself (coordinate data of 4 marker points in local coordinate system), then the transformation matrix and translation matrix between two sets of coordinate data were established. Finally, the coordinate data (probe-tip's coordinates)

310 of the bony-markers (also known as anatomical feature points) was obtained. According to the
311 coordinate data of the Marker points on the thigh and calf respectively in the calibration of bony-
312 markers and ground reference points, the transformation matrix and the translation matrix between
313 the two sets of coordinate data were established, it was used to calculate the coordinate data of
314 bony-markers points in the calibration of ground reference points. Finally, according to the
315 coordinate data of Marker point on the leg in the calibration of ground reference point and the
316 coordinate data during the movement of human lower limb, the transformation matrix and
317 translation matrix between the two sets of coordinate data were established. Thereby, the
318 coordinate data of the bony-markers in the lower limb movement of the human body was
319 obtained.



320

321

Fig. 10 The probe and its local coordinate system

322

Establishment of local coordinate system of femur and tibia

323

This study defines and establishes the local coordinate system of the femur and tibia according to

324

the seven bony-markers of the lower extremities. In 1983, Grood et al. [26] first introduced the

325

method of establishing the joint coordinate system for the three-dimensional motion of joints.

326 Later, other scholars redefined the method of establishing the local coordinate system of various
327 parts of the human body [27-31]. Dane et al. [32] modified the coordinate system definition
328 method proposed by Grood. Of course, some scholars have proposed the definition method of the
329 coordinate system of human lower limbs and knee joints [2]. This paper refers to the above
330 scholars' research and establishes the human femur and tibia local coordinate system in
331 combination with the actual situation. As shown in **Fig. 11**, the femur and tibia coordinate systems
332 are established. The method is as follows:

333 The local coordinate system of the femur: the line connecting the lateral femoral condyle and
334 medial femoral epicondyle is the X axis, the direction is pointing to the outside, and the midpoint
335 of the line is the origin. The X-axis multiplied by the line being connected the femur greater
336 trochanter and the origin to obtain the Y-axis with the direction facing forward. The X-axis
337 multiplied by the Y-axis to obtain the Z-axis with the direction facing up.

338 The local coordinate system of the tibia: the connection between the medial and lateral tibial
339 plateau is the X axis, the direction is pointing to the outside, the midpoint of the line is the origin,
340 and the X-axis multiplied by the line being connected the origin and the midpoint of the inner and
341 outer ridges to obtain the Y-axis, the direction is forward. The X-axis multiplied by the Y-axis to
342 obtain the Z-axis with the direction facing up.

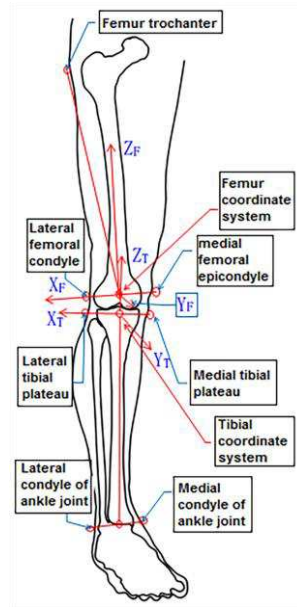


Fig. 11 Knee joint femur and tibia local coordinate system

343

344

345 Solving knee kinematic parameters

346 According to the above method, the local coordinate systems of femur and tibia were established

347 according to the bony-markers [33]. The femoral coordinate system was rotated and translated to

348 obtain the tibia coordinate system. According to the order of coordinate rotation,

349 coordinates transform can be divided into two categories [18]. One type is that the three axes

350 were different for the three rotation transforms to rotate, the other type is that the first and third

351 rotations axes are the same one, and these two types all have six rotation transformation orders.

352 In this paper, the order of X-Y-Z is used for Euler rotation, and its transformation matrix is R:

$$353 \quad R = \begin{bmatrix} R_{11} & R_{12} & R_{13} \\ R_{21} & R_{22} & R_{23} \\ R_{31} & R_{32} & R_{33} \end{bmatrix} \quad (1)$$

354 The femoral coordinate system were orderly rotated α angle around the X axis, rotated β angle

355 around the Y axis, rotated γ angle around the Z axis, and coincides with the tibia coordinate

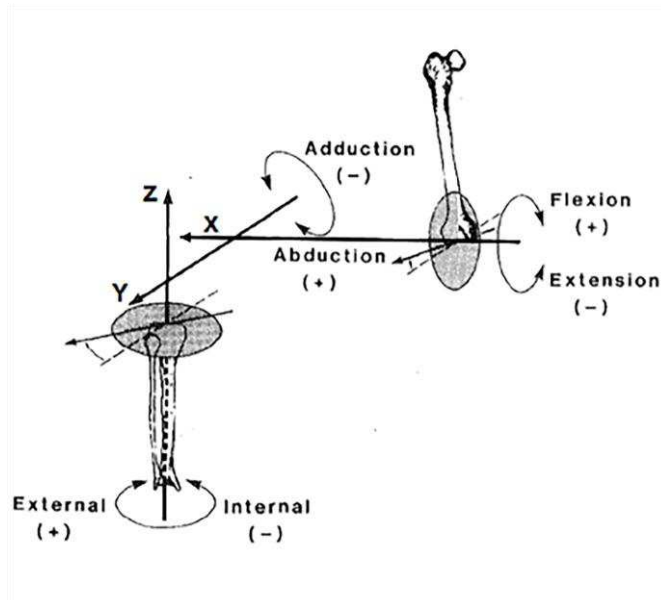
356 system. According to the coordinate transformation principle, the rotation transformation matrix R

357 is as follows:

$$358 \quad \begin{cases} \alpha = a \tan 2(-R_{32}, R_{33}) \\ \beta = a \tan 2(R_{31}, \sqrt{R_{11}^2 + R_{12}^2}) \\ \gamma = a \tan 2(-R_{21}, R_{11}) \end{cases} \quad (2)$$

$$359 \quad a \tan 2(x, y) = a \tan(x / y)$$

360 According to the local coordinate system, the follows were respectively defined: the flexion
361 extension angle of the femur relative to the tibia is the angle α of the femoral coordinate system
362 rotating around the X axis, and the adduction abduction angle is the angle β of the femoral
363 coordinate system rotating around the Y axis. The internal and external rotation angle is the angle
364 γ of the femoral coordinate system rotating around the Z axis, as shown in Figure 12 below .The
365 kinematic parameters of the knee joint during the lower limb movement are obtained by
366 calculating the α , β and γ angle.

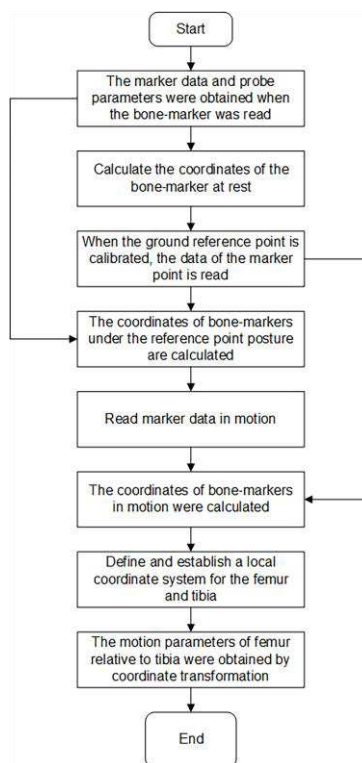


367

368 **Fig. 12** Joint angles are defined by rotations occurring about the three joint coordinate axes.

369 **Figure 13** is the flow chart of the main program for obtaining relative motion parameters of
370 femoral-tibial joint, which were programed in MATLAB. The program starts reading the data by

371 calculating the coordinates of the bony-markers firstly. Secondly, marker data when the
 372 reference-points were calibrated is read and the coordinates of the bony-markers under the
 373 reference point posture were calculated, then the marker data in the motion is read to calculate the
 374 coordinates of bony-markers in the movement; At the meantime, the local coordinate system of
 375 the femur and tibia were established according to the bony-markers. Finally the coordinate
 376 transformation was used to solve the kinematic parameters of the knee joint.



377

378 **Fig. 13** Main program flow chart of obtaining relative motion parameters of femoral tibial joint

379 **Abbreviations**

380 TKA: total knee arthroplasty;

381 **Acknowledgements**

382 Not applicable.

383 **Authors' contributions**

384 WJP designed the study, performed the measurements in healthy subjects, analyzed the data,
385 and drafted the manuscript. WSH, ZX, HH, WYQ, LJJ, CX and LY participated in performing the
386 measurements of healthy subjects, analyzing the data, and drafting the manuscript. All authors
387 read and approved the final manuscript.

388 **Funding**

389 This investigation was funded by a grant from the National Institutes of Health and supported
390 by National Natural Science Foundation of China (31370999). (Information for disclosures can
391 be taken from the online abstract system after entering all authors.

392 **Availability of data and materials**

393 The datasets used and/or analyzed during the current study are available from the
394 corresponding author on reasonable request.

395 **Ethics approval and consent to participate**

396 All subjects provided written informed consent prior to their participation in the study.

397 **Consent for publication**

398 All authors confirmed the consent for publication.

399 **Competing interests**

400 The authors declare that they have no competing interests.

401 **Author details**

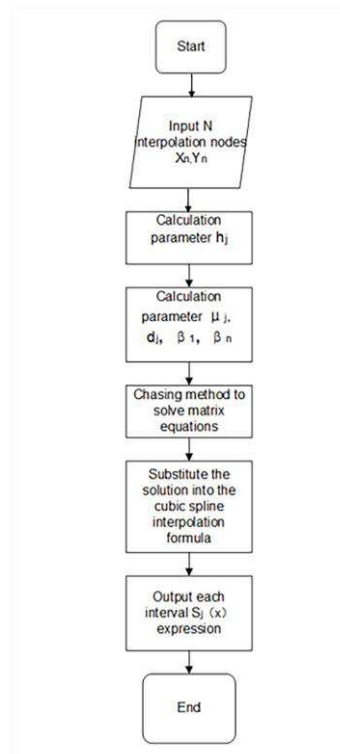
402 ¹School of Mechanical and Power Engineering, Henan Polytechnic University, Jiaozuo
403 454000, China

404 ²Shanghai Sixth People's Hospital, Shanghai 200233, China.

405 ³Medical University, Qiqihar 161006 , Heilongjiang Province, China. School of medical
406 technology.

407 ⁴The First Affiliated Hospital of Henan Polytechnic University, Jiaozuo 454000, Henan
408 Province, China.

409 Appendix 1 Cubic spline interpolation function principle



410

411 **Figure 14** Block diagram for solving cubic spline interpolation function

412 The block diagram for solving cubic spline interpolation function is shown in **Fig. 14**. The cubic
413 spline interpolation function can be solved according to definitions and boundary conditions.

414 Given some data point correspondence function values in the interval $[a, b]$, $\{x_1, x_2, \dots, x_n\}$,

415 corresponding function value $\{y_1, y_2, \dots, y_n\}$, $S(x)$ is a cubic spline interpolation function, which

416 satisfies $S(x_j) = y_j (j = 1, 2, \dots, n)$ and has a second-order continuous derivative on $[a, b]$. $S(x)$

417 determines a cubic polynomial on each subinterval $[x_j, x_{j+1}]$, known

418 $S''(x_j) = M_j, S''(x_{j+1}) = M_{j+1}, h_j = x_{j+1} - x_j (j = 1, 2, \dots, n-1)$, then

419
$$S(x) = \frac{(x_{j+1} - x)^3}{6h_j} M_j + \frac{(x - x_j)^3}{6h_j} M_{j+1} + \left(y_j - \frac{M_j}{6} h_j^2 \right) \frac{x_{j+1} - x}{h_j} + \left(y_{j+1} - \frac{M_{j+1}}{6} h_j^2 \right) \frac{x - x_j}{h_j}, \quad (1)$$

420 The system of equations in matrix form were solved finally according to known conditions.

421
$$\begin{bmatrix} 2 & 1 & & & \\ \mu_2 & 2 & 1 - \mu_2 & & \\ & \cdot & \cdot & \cdot & \\ & & \mu_{n-1} & 2 & 1 - \mu_{n-1} \\ & & & 1 & 2 \end{bmatrix} \begin{bmatrix} M_1 \\ M_2 \\ \cdot \\ M_{n-1} \\ M_n \end{bmatrix} = \begin{bmatrix} \beta_1 \\ d_2 \\ \cdot \\ d_{n-1} \\ \beta_n \end{bmatrix} \quad (2)$$

422
$$\mu_j = \frac{h_{j-1}}{h_{j-1} + h_j}, d_j = 6 \left(\frac{y_{j+1} - y_j}{h_j} - \frac{y_j - y_{j-1}}{h_{j-1}} \right) \frac{1}{h_{j-1} + h_j},$$

423
$$\beta_1 = \frac{6}{h_1} \left(\frac{y_2 - y_1}{h_1} - y_1' \right), \beta_n = \frac{6}{h_{n-1}} \left(y_n' - \frac{y_n - y_{n-1}}{h_{n-1}} \right),$$

424 The coefficient matrix of equation (2) is a three-diagonal matrix and a diagonally dominant
 425 matrix, so there is a unique solution. The interpolation function $S(x)$ on $[a, b]$ is obtained by taking
 426 the solution into equation (1).

427 **References**

428 1. Liu HT, Zhao Z, Wu X, Qiang H & Zhang YY. The imaging measurement of KBD knees and its
 429 clinical significance. *Annals of anatomy*, 2014; 196: 167-168.

430 2. Berger RA, Rosenberg AG, Barden RM, Sheinkop MB, Jacobs, JJ, & Galante, JO. Long-term
 431 followup of the Miller-Galante total knee replacement. *Clinical Orthopaedics and Related*
 432 *Research*, 2001;388: 58-67.

433 3. Xinhua Z, Min W, Chao L, Liang Z, & Yixin Z. Total knee arthroplasty for severe valgus knee
 434 deformity. *Chinese Medical Journal*, 2014; 127(6): 1062-1066.

435 4. Rafi, A. Motion capture and computer arts. *International Journal of Arts &*
 436 *Technology*, volume 2008; 1(1): 1-12(12).

- 437 5. Livne M, Sigal L, Brubaker M, & Fleet D. Walking on Thin Air: Environment-Free
438 Physics-Based Markerless Motion Capture. 2018 15th Conference on Computer and Robot
439 Vision (CRV). IEEE Computer Society, 2018.
- 440 6. Arendra A, & Akhmad S. Development of esmoca biomechanic, motion capture
441 instrumentation for biomechanics analysis. Journal of Physics Conference.2018; 953.
- 442 7. Karatsidis A, Bellusci G, Schepers HM, Zee MD, Andersen MS, Veltink PH. Estimation of
443 Ground Reaction Forces and Moments During Gait Using Only Inertial Motion Capture.
444 Sensors, 2017; 17(1):75.
- 445 8. Labbe DR, Hagemester N, Tremblay M, & Guise JD. Reliability of a method for analyzing
446 three-dimensional knee kinematics during gait. Gait and Posture, 2008; 28(1):170-174.
- 447 9. Saboune J, Charpillat F. Using interval particle filtering for marker less 3D human motion
448 capture. Tools with Artificial Intelligence, 2005. ICTAI 05.17th IEEE International Conference
449 on IEEE.2005.
- 450 10. Schmitz A , Ye M, Boggess G. , Shapiro R, Yang R , & Noehren B. The measurement of in vivo
451 joint angles during a squat using a single camera markerless motion capture system as
452 compared to a marker based system. Gait & Posture, 2015; 41(2):694-698.
- 453 11. Clement, Julien, Hagemester N, Aissaoui R, & De Guise, J A. Comparison of quasi-static and
454 dynamic squats: a three-dimensional kinematic, kinetic and electromyographic study of the
455 lower limbs. Gait & Posture, 2014; 40(1):94-100.
- 456 12. Riener R, Rabuffetti, M, & Frigo, C. Stair ascent and descent at different inclinations. Gait and
457 Posture, 2002; 15(1): 32-44.
- 458 13. Fu, YC, Simpson, KJ, Msph, TLK, & Mahoney, OM. Does interlimb knee symmetry exist after
459 unicompartmental knee arthroplasty? Clinical Orthopaedics and Related Research, 2013;
460 471(1):142-149.
- 461 14. Kowalk DL, Duncan JA, Vaughan CL. Abduction-adduction moments at the knee during stair
462 ascent and descent. Journal of Biomechanics, 1996; 29(3): 383- 388.

- 463 15. Gang T, Gao-Feng W, Hai Z, Shi-Lei L, Wen-Ting Ji , & Dong-Mei. Measurement and analysis
464 of the joint angle in lower limb during stair ascent. *Medical Biomechanics*, 2011; 26(5):
465 460-464.
- 466 16. Yutao XU , Weijie W , Teng XU, Jiawei L I , Yixuan, D , & Hao D. Study on the characteristics of
467 left and right ankle joints in vicon motion capture system during human walking. *Modern
468 information technology*, 2018; 2(06):7-9+12.
- 469 17. Tang G, Cheng RS, HU Xiong, Zhang BY, and Wu G. Design of human knee dynamics
470 simulation platform based on Matlab. *Journal of Donghua University (Nature Science)*, 2016;
471 42(05):725-731.
- 472 18. Dooley E, Carr J, Carson E, & Russell S. The effects of knee support on the sagittal
473 lower-body joint kinematics and kinetics of deep squats. *Journal of Biomechanics*.2018.
- 474 19. Guo Y, Zhang XS, An MW, Chen WY. Determination of quadriceps forces in squat and its
475 application in contact pressure analysis of knee joint. *Acta Mechanica Solida Sinica* 2012; 25:
476 53-60.
- 477 20. Wu S, Zhang Q, Xiao BX, Wei XP. A New Data Processing Method for Optical Motion Capture.
478 *Computer Applied Research* 2009; 26(05).
- 479 21. Alonso FJ, DelCastillo JM, Pintado P. Motion data processing and wobbling mass modeling in
480 the inverse dynamics of skeletal models. *Mechanism and Machine Theory* 2006; 8(6):1-17
- 481 22. Liu G , Mcmillan L. Estimation of missing markers in human motion capture. *The Visual
482 Computer* 2006; 22(9):721-728.
- 483 23. Liu YH, Feng Y, Li QB, Wan YW, Luo CG, Luo J. Study on Kinematics Parameter Characteristics
484 of Stilt-walking Method Based on Three-dimensional Motion Capture Technology. *Journal of
485 Beijing University of Traditional Chinese Medicine* 2018; 41(03):235-241.
- 486 24. Schmidt R, Disselhorst-Klug C, Silny J, & Günter Rau. A marker-based measurement
487 procedure for unconstrained wrist and elbow motions. *Journal of Biomechanics*, 1999; 32(6):
488 615- 621.

- 489 25. Xu XY, Zhong TY. Cubic spline interpolation function construction and Matlab
490 implementation. *Ordnance automation*. 2016; (11):76-78.
- 491 26. Grood ES, Suntay WJ. A joint coordinate system for the clinical description of
492 three-dimensional motions: application to the knee. *Journal of Biomechanical Engineering*
493 1983;105: 136- 44.
- 494 27. Wu G, et al ISB recommendation on definitions of joint coordinate system of various joints
495 for the reporting of human joint motion- part I: ankle, hip, and spine .International Society
496 of Biomechanics. *Journal of Biomechanics*, 2002; 35(4): 543- 548.
- 497 28. Wang JP, Zhang LL, Wang CT. Relative motion analysis of patellofemoral joint of human knee.
498 *Journal of Shanghai Jiaotong University* 2009; 43(07):1043-1046.
- 499 29. Wang JP, Han XL, Ji WT, Wang CT. Three-dimensional image registration analysis of relative
500 motion of human knee-tibiofemoral joint. *Journal of biomedical engineering* 2009;
501 26(06):1340-1344.
- 502 30. Wu G, Helm FCTVD, Veeger HEJ. ISB recommendation on definitions of joint coordinate
503 systems of various joints for the reporting of human joint motion—Part II: shoulder, elbow,
504 wrist and hand. *Journal of Biomechanics* 2005; 38(5):981-992.
- 505 31. Amadi HO, Majed A, Emery RJH, et al (2010) A humeral coordinate system for in vivo 3-D
506 kinematics of the glenohumeral joint. *Journal of Musculoskeletal Research* 2010;
507 12(03):169-174.
- 508 32. Dabirrahmani D, & Hogg M. Modification of the grood and suntay joint coordinate system
509 equations for knee joint flexion. *Medical Engineering and Physics* 2016; 39: 113- 116.
- 510 33. Even-Tzur, Gilad. Invariance property of coordinate transformation. *Journal of Spatial Science*,
511 2017; 1-12.

Figures

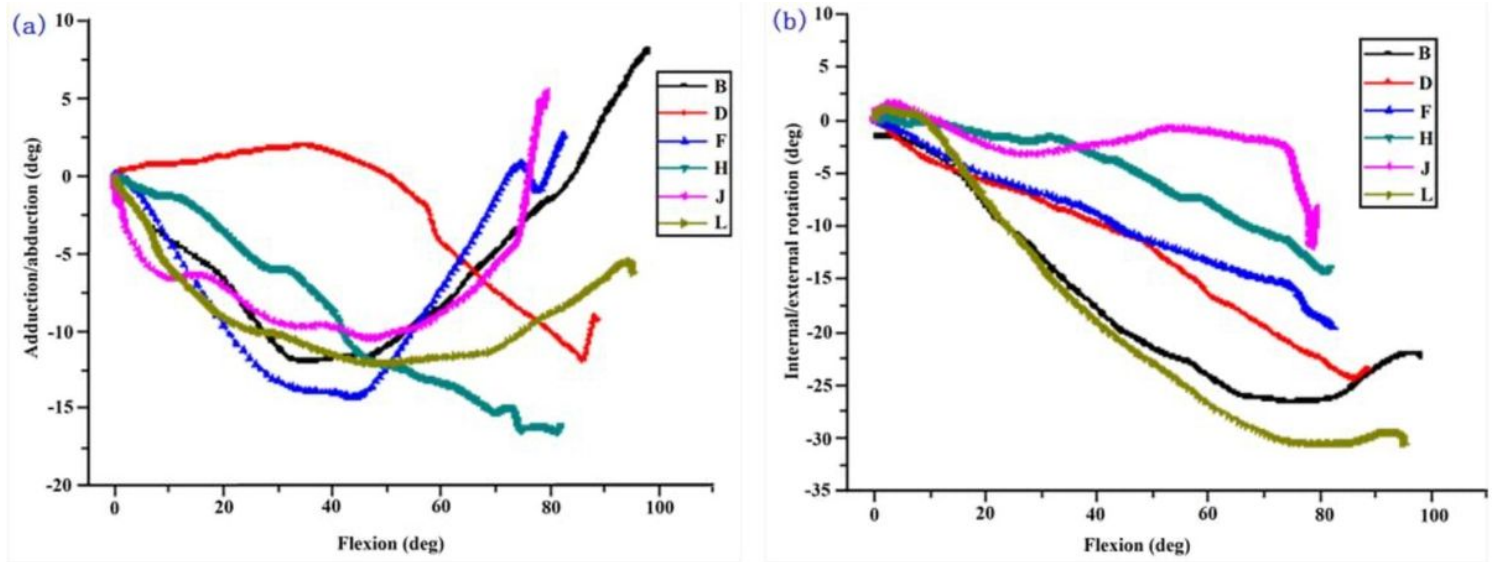


Figure 1

(a) The relative rotation motion of femur vs tibia under different flexion during squat (abduction/adduction). (b) The relative rotation motion of femur vs tibia under different flexion during squat (internal/external rotation)

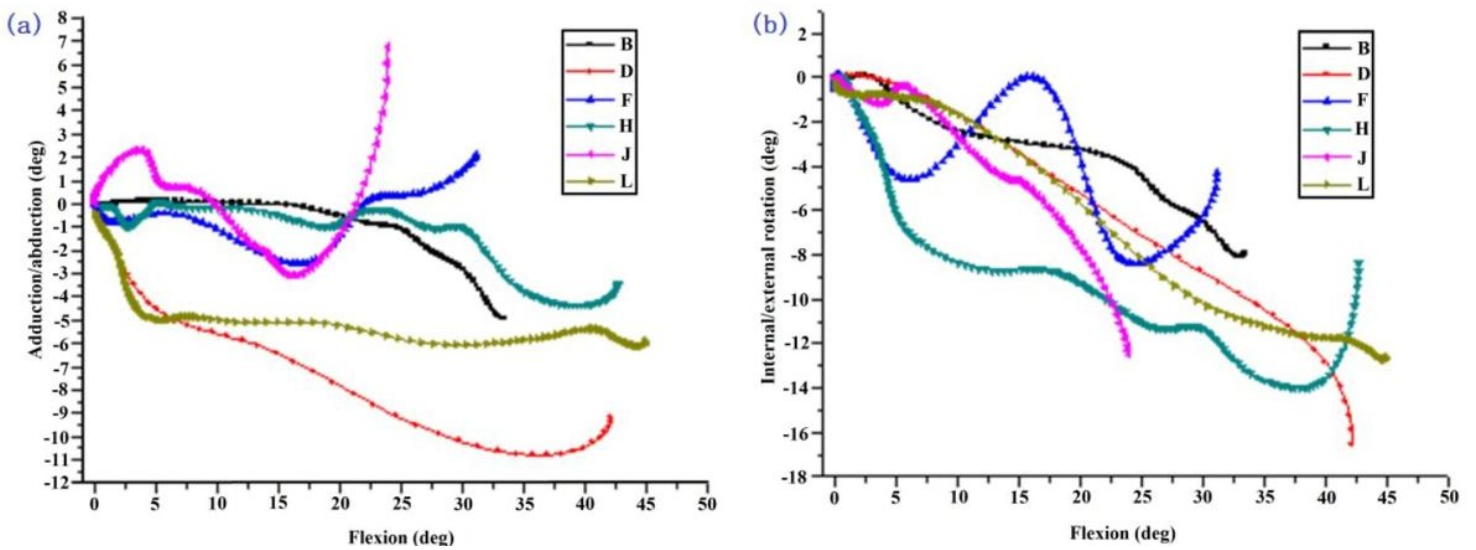


Figure 2

(a) The relative rotation motion of femur vs tibia under different flexion during upstairs climbing (abduction/adduction). (b) The relative rotation motion of femur vs tibia under different flexion during upstairs climbing (internal/external rotation)



Figure 3

Position sensors of motion capture system

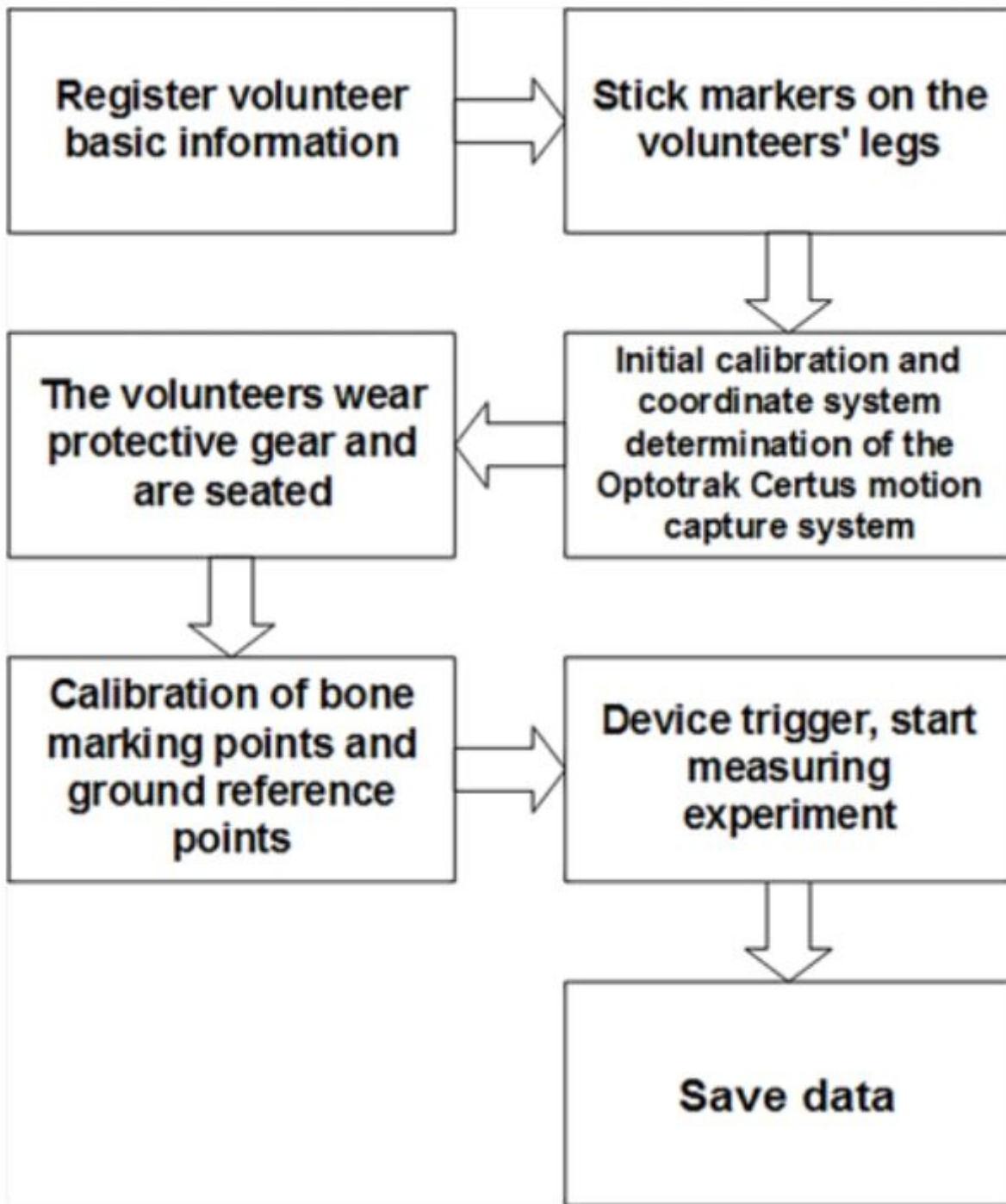


Figure 4

Motion capture measurement flow chart

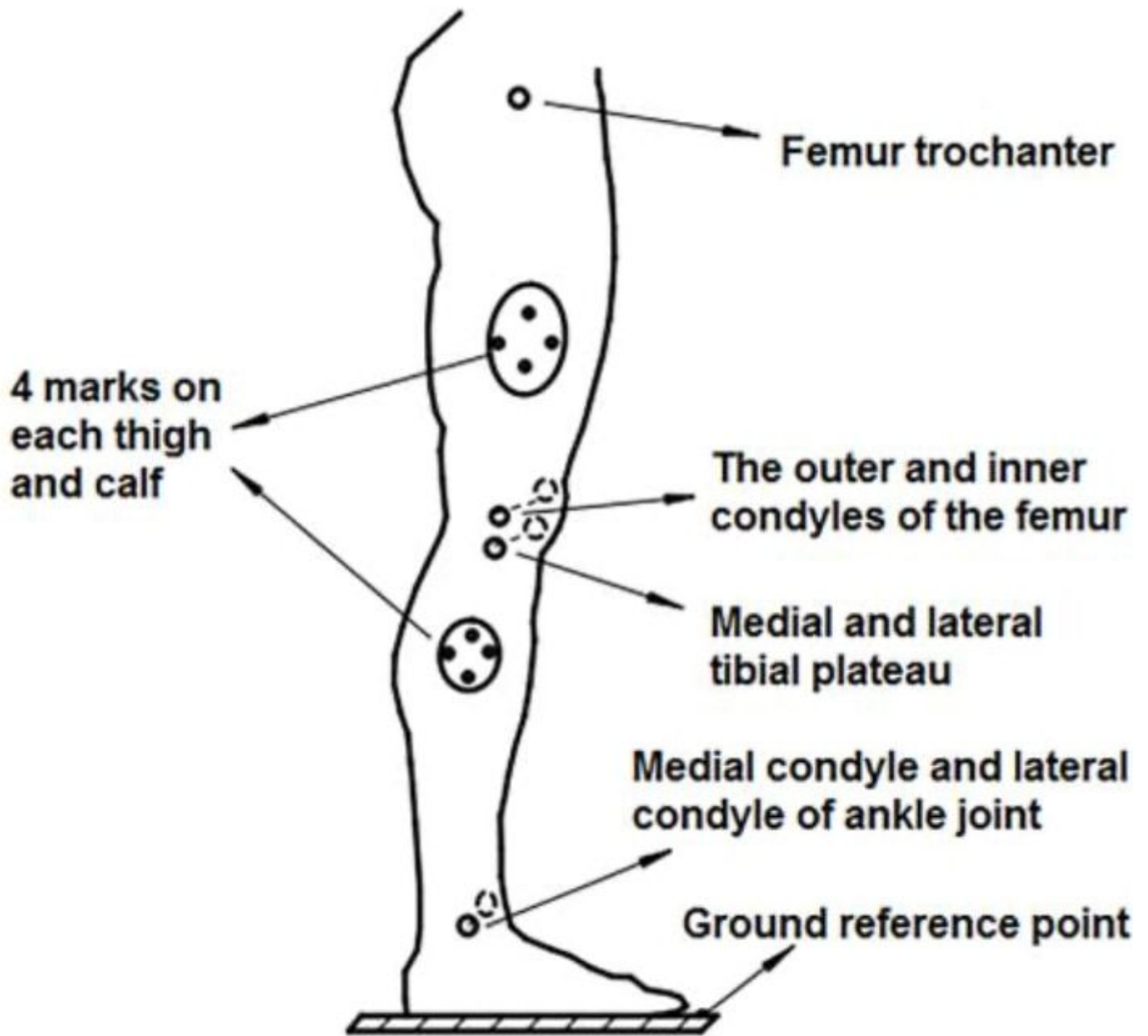


Figure 5

The position of Markers and anatomic feature points in human lower extremity

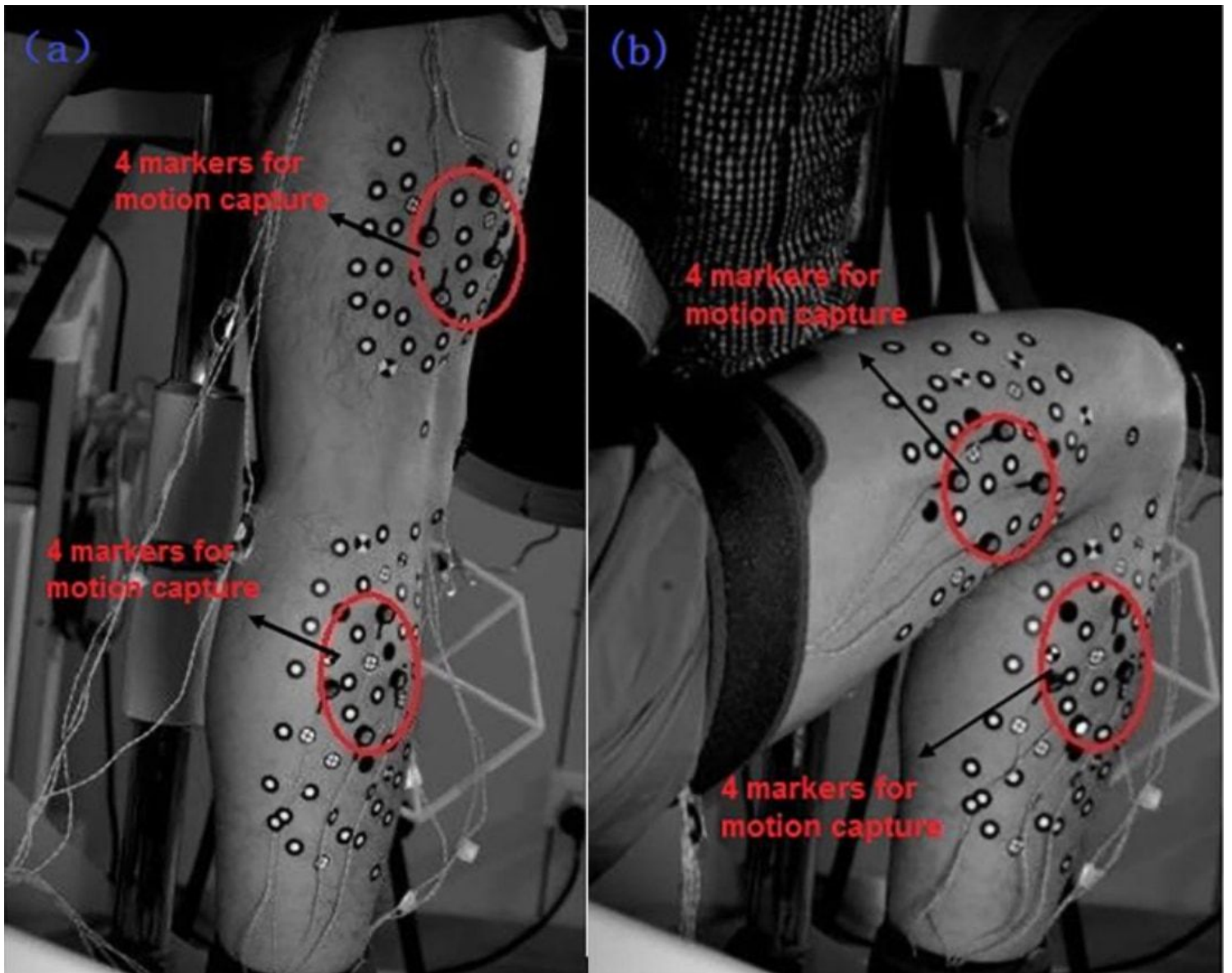


Figure 6

(a) Site Map of Squatting Motion Measurement (orthostatism). (b) Site Map of Squatting Motion Measurement (maximum of knee joint flexion)

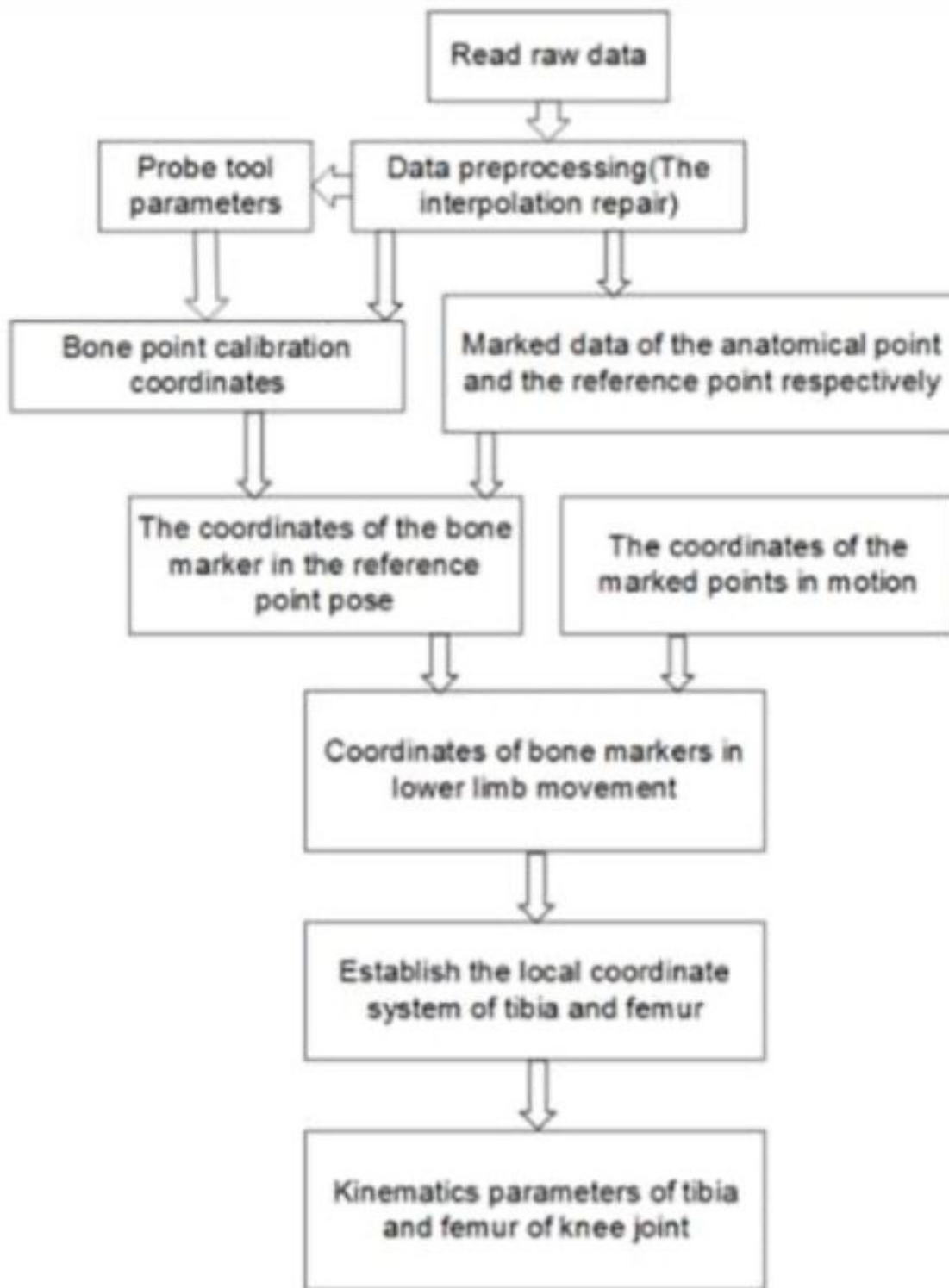


Figure 7

Data processing flow chart

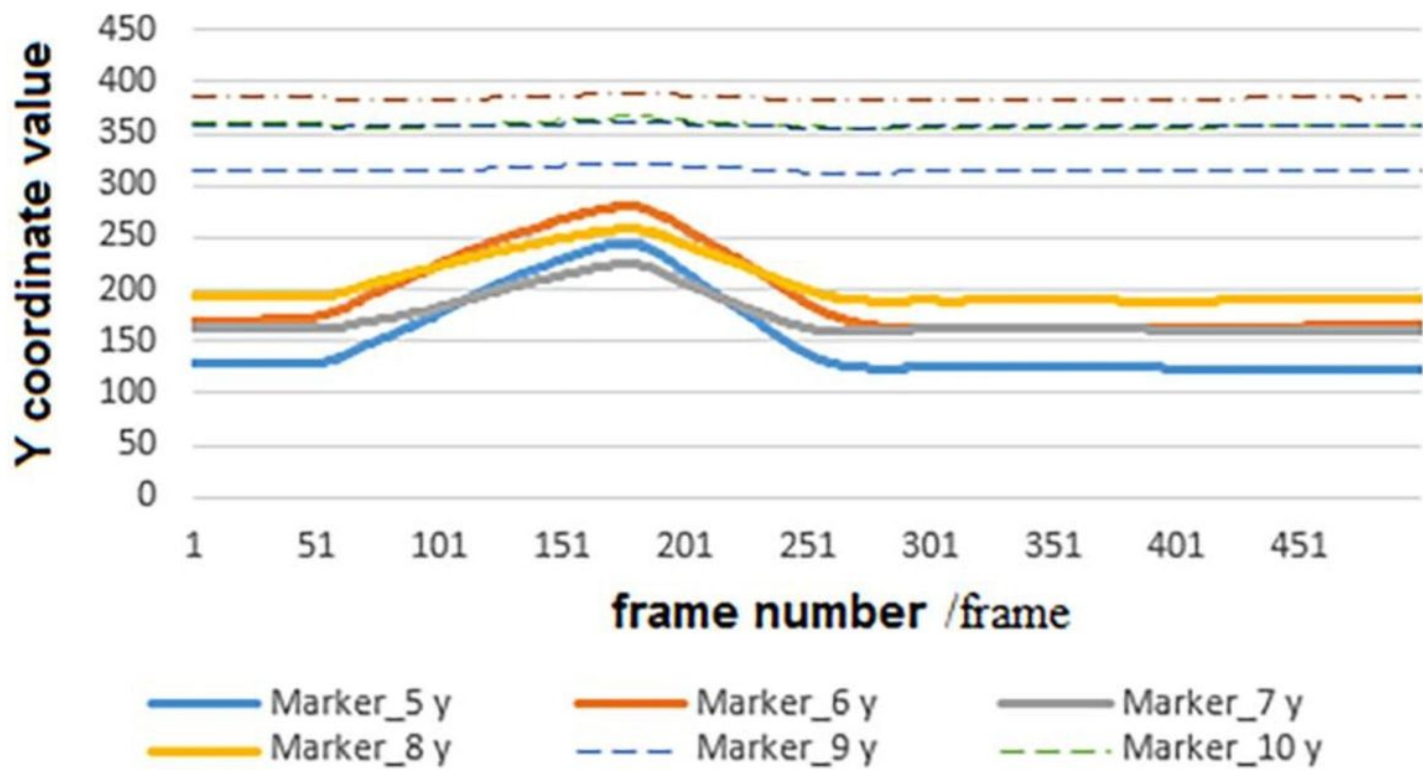


Figure 8

The coordinate values in Y direction of markers in thigh and shank in a squat

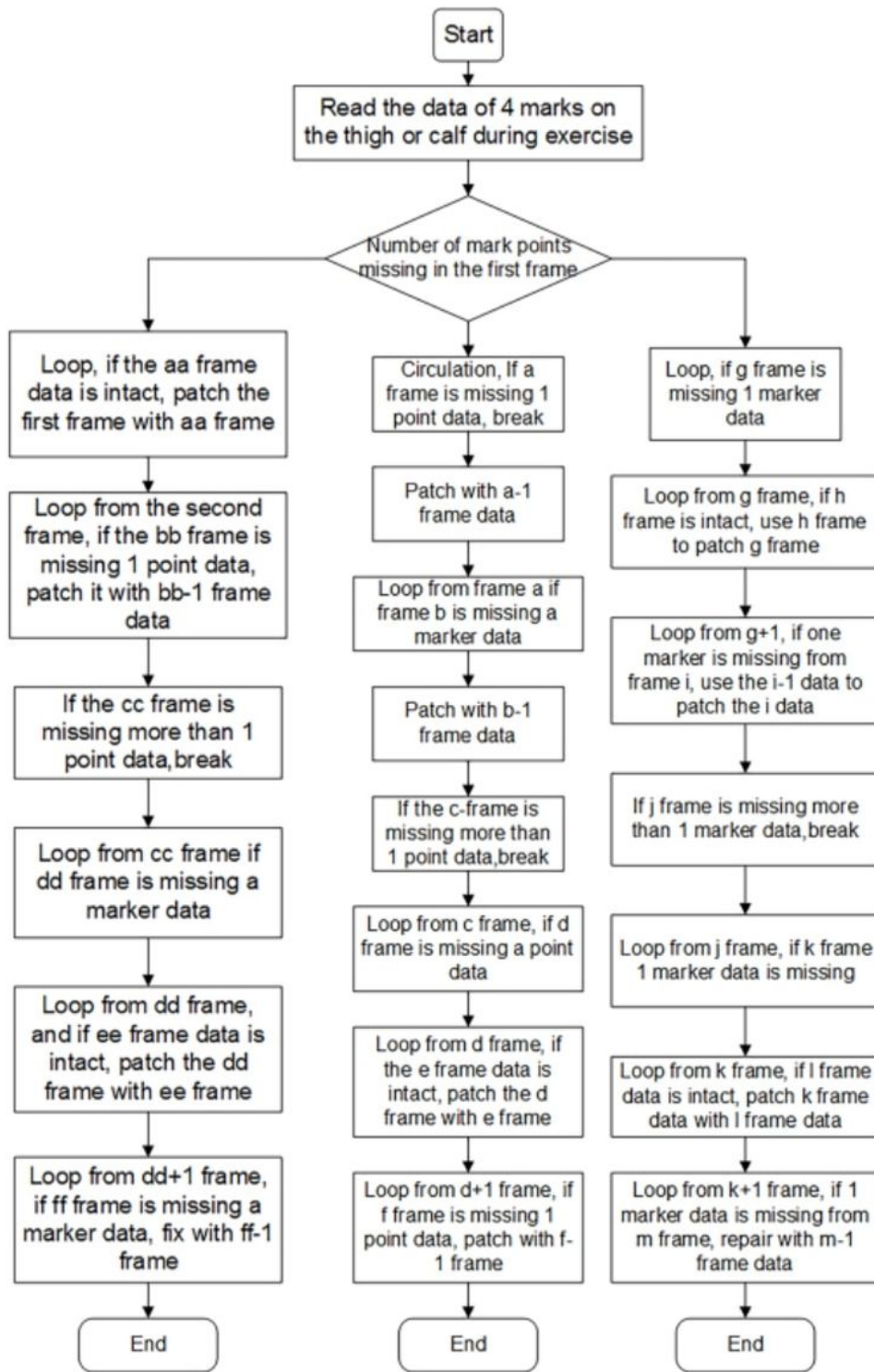


Figure 9

Patch program flow chart

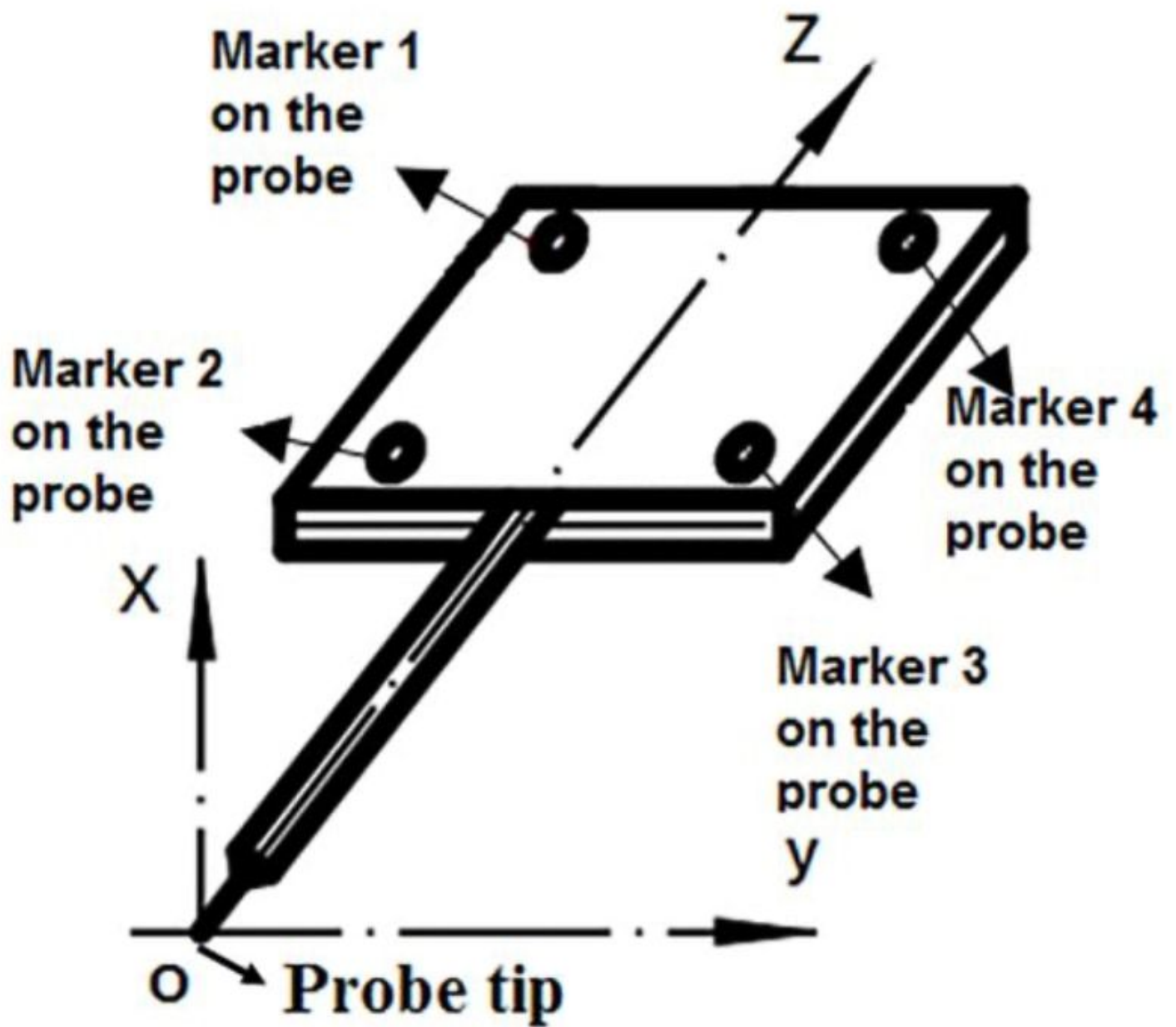


Figure 10

The probe and its local coordinate system

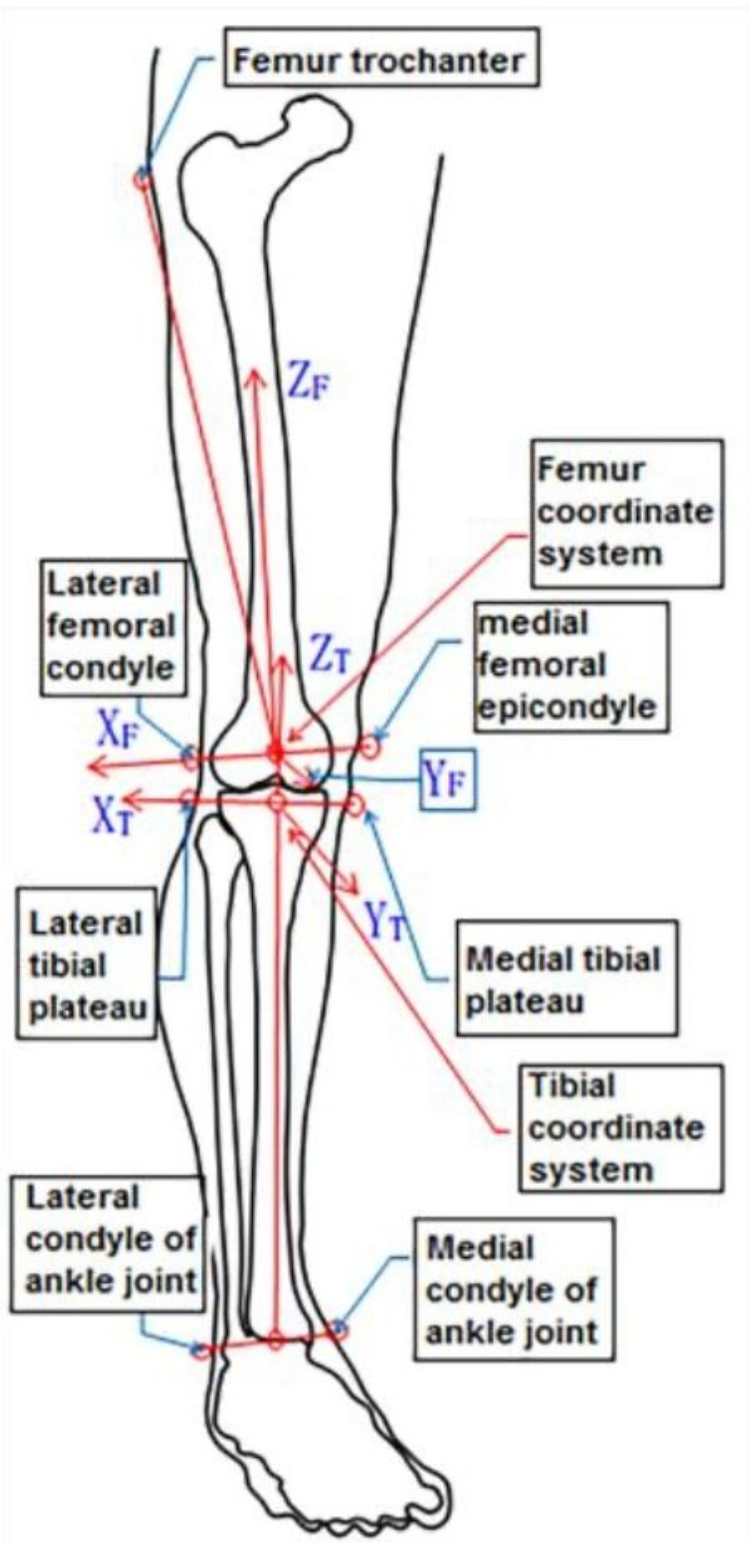


Figure 11

Knee joint femur and tibia local coordinate system

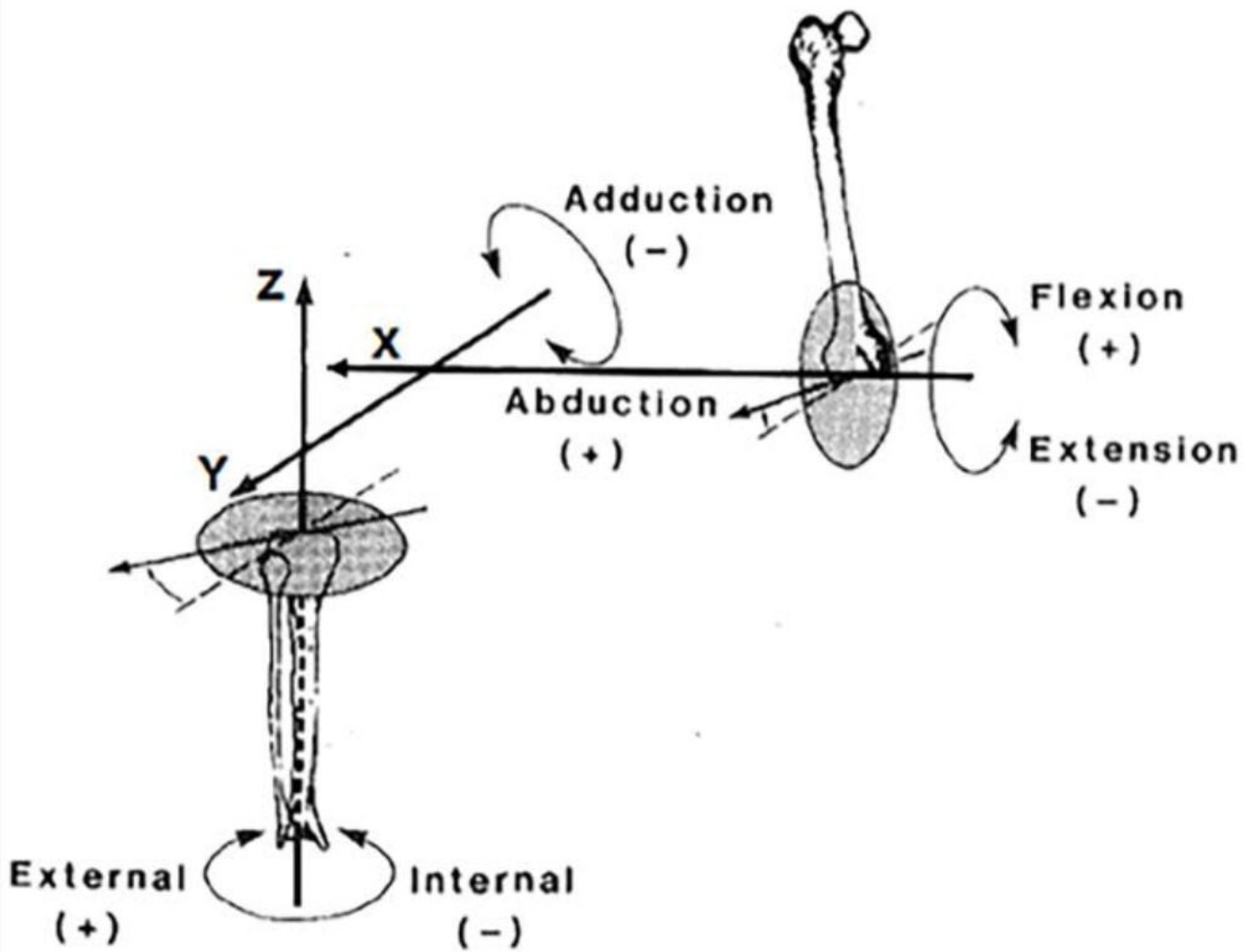


Figure 12

Joint angles are defined by rotations occurring about the three joint coordinate axes.

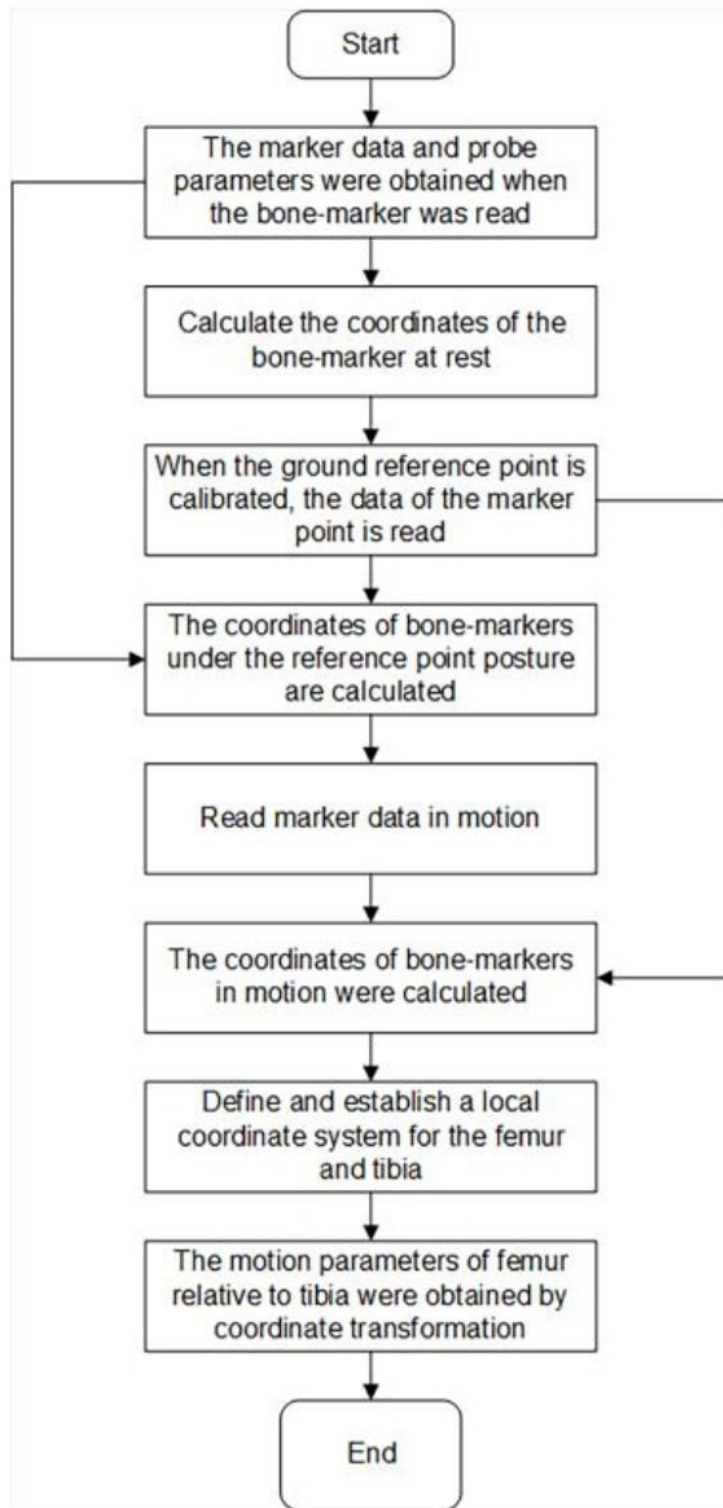


Figure 13

Main program flow chart of obtaining relative motion parameters of femoral tibial joint